Synthesis and magnetic-electronic characterization of mixed-valence $LuFe_2O_{4-\delta}$: effect of stoichiometry δ

M A Peck[1, 2], W N Sibanda[1], G Diguet[1], C Martin[3], E Carleschi[1] and G R Hearne[1]

[1]Department of Physics, University of Johannesburg, PO Box 524, Auckland Park, 2006, South Africa
[2]Department of Chemistry, University of Johannesburg, PO Box 524, Auckland Park, 2006, South Africa
[3]Laboratoire CRISMAT, ENSICAEN, UMR 6508 CNRS, Caen, France

Email: adlipeck@gmail.com

Abstract. Samples of $LuFe_2O_{4-\delta}$ of varying oxygen stoichiometry (δ), prepared by solid state synthesis, have been characterised by x-ray diffraction, ^{57}Fe Mössbauer-effect spectroscopy, SQUID magnetometry and transmission electron spectroscopy as well as electron-diffraction analysis. Magnetisation measurements show that the onset of ferrimagnetic ordering is confined to 245-250 K for the synthesised samples. Detailed analysis of Mössbauer spectra measured at variable cryogenic temperature confirm the mixed valence state and reveal the effects of charge and spin frustration of the triangular network of Fe atoms. The electron diffraction analysis demonstrates the existence of charge ordered superstructure (satellites) as well as an inhomogeneous distribution of oxygen throughout the lattice, irrespective of the δ values.

1. Introduction

Multifunctional materials able to combine both magnetism and ferroelectric polarization, termed multiferroics, have strong potential for novel electronic functional devices [1]. This magneto-electric coupling offers manipulation of the electric polarization via a magnetic field and vice versa [2]. Rare-earth ferrites (RFe_2O_4) have been shown to exhibit this phenomenon, with a great deal of emphasis towards lutetium ferrite ($LuFe_2O_4$) since Ikeda *et al.* showed the existence of a mixed-valence superstructure, Fe^{2+}/Fe^{3+} charge-ordering (CO), within these compounds [3]. There were initial claims that the CO is intimately linked to ferroelectric properties; however this has now been refuted and the electric polarization is now considered to be an extrinsic effect [4].

A review by Angst [4] highlights that due to the frustrated $LuFe_2O_4$ lattice system, the triangular network of Fe atoms contains a number of degenerate charge and spin ordered states allowing transitions in both the magnetic and electric ordered dimensions. It has also been reported that oxygen-stoichiometry, $LuFe_2O_{4\pm\delta}$, plays a critical role in varying the physical and structural properties of this material. Both excess ($\delta > 0$) [5, 6] and deficient ($\delta < 0$) [7] samples lead to a suppression of the magnetic ordering volume and temperature (T_N) as well as a deformation of the structural lattice. The mechanism of this variation as a function of the absence or excess of oxygen is still not fully understood. In this paper we will report on the synthesis and magnetic-electronic characterization of three oxygen-varied $LuFe_2O_{4+\delta}$ samples and compare our results to those reported for excess and stoichiometric samples.

$LuFe_2O_4$ crystallizes in a rhombohedral lattice, consisting of an alternation of LuO_6 monolayers with triangular networked FeO_5 bi-layers (figure 1(a)), where Fe-O co-ordinates in a trigonal bipyramidal structure as indicated in figure 1(c), characteristic of these rare-earth ferrites [4]. Using high resolution transmission electron microscopy (TEM) and electron diffraction (ED) for samples with $\delta < 0$ Yang *et al*. observed that a structural modulation occurred as well as local distortions in the *b-c* plane and deformation of the FeO_5 polyhedron, presumably affecting magnetic transitions [7]. A similar disruption of the stoichiometric lattice was observed by Hervieu *et al*. for samples where $\delta > 0$, in which case the cationic system expands to accommodate excess oxygen (up to $\delta = 0.5$), resulting in a loss of the rhombohedral layer-stacking [5]. Their results point towards a reversible oxygen-storage application of $LuFe_2O_4$ as well as the possibility to fine-tune $\delta > 0$. Previous Fe Mössbauer spectroscopy results show that Fe^{3+}/Fe^{2+} CO occurs below an onset temperature of $T_{CO} = 320$ K [8] and above 370 K electron-hopping, $Fe^{2+} \leftrightarrow Fe^{3+}$, destroys the mixed-valence superstructure (CO melting) [9]. Stoichiometric samples show a paramagnetic to ferrimagnetic transition at $T_N \approx 250$ K [8, 9] whilst off-stoichiometric samples show a suppression of T_N to below 250 K [5-7]. An antiferrimagnetic transition also occurs at 175 K for all samples, while only off-stoichiometric samples display spin-glass magnetic behaviour at lower temperatures, $T_{LT} < 175$ K [6, 7].

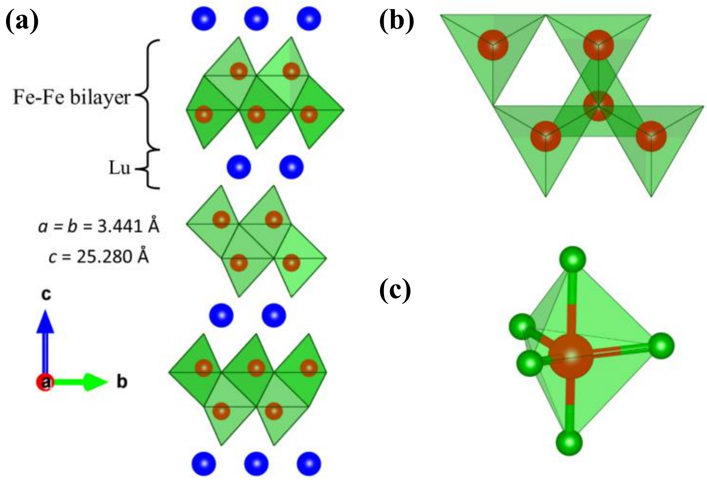

Figure 1 (colour online): (a) Rhombohedral lattice, *R3-m,* of $LuFe_2O_4$ viewed in the *b-c* plane (b) View down the *c*-axis of a single bilayer showing the triangular network of Fe atoms. (c) Five-fold coordination of Fe-O. Lu atoms are shown in blue, Fe in red and O atoms, at the vertices of the trigonal bipyramid, are shown in green.

2. Experimental

Two $LuFe_2O_4$ polycrystalline powdered samples, enriched to 10 - 14% ^{57}Fe, were prepared by solid-state reaction of starting mixtures according to the stoichiometric ratio $0.50Lu_2O_3$: $0.83Fe_2O_3$: $0.34Fe$. Mixtures were thoroughly ground in an agate mortar, pestled and compressed into 20 mg and 100 mg pellets. The pellets were vacuum-sealed in a quartz ampoule to 3×10^{-6} mbar before heating at 1100 °C for 12 hrs. A third sample with $\delta \approx 0$ (designated MP), prepared on a gram-scale via a similar method, was received from Martin's group at the *Laboratoire Crismat, Caen, France* [5, 10]. This was also characterized and compared to our two synthesized samples.

Structural characterization was performed on synthesized samples by X-ray powder diffraction (XRPD) using a *Phillips X-Pert Pro* instrument with Cu-K_α radiation. Magnetic susceptibility measurements were carried out in a SQUID (QD: MPMS) in the temperature range 150 – 300 K. ^{57}Fe Mössbauer effect spectroscopy (MES) measurements in transmission mode were conducted using a 10 mCi $^{57}Co(Rh)$ source and all samples were characterized with respect to a 25 μm α-Fe-foil reference. Low temperature measurements were performed in a top-loading cryostat with the source and sample at the same temperature.

In addition electron diffraction measurements were performed on micron-dimensioned grains in a TEM, similar to those indicated in references [5, 10].

3. Results and discussion

3.1. XRPD

Of the two synthesized samples, the diffraction pattern for the 20 mg sample showed a significant amount of impurities, (indicated by arrows in figure 2(b)) relative to the 100 mg sample. Sample MP's diffraction pattern (not shown here, see reference [5]) showed no discernible impurity phases either. Since sample MP was produced on a gram-scale, a possible inverse proportionality mass-purity effect takes place leading to unreacted material. This can also be observed in the Mössbauer spectrum of the 20 mg sample (figure 2(c)), which shows evidence of remnant Fe_3O_4 and Fe impurity phases (as indicated by arrows) from the reaction sequence, not observed in the MP and 100 mg samples (see figure 3).

The crystal structure was resolved by Rietveld refinement and a best-fit, rhombohedral cell, with *R3-m* space group was obtained with parameters $a = b = 3.441$ Å and $c = 25.280$ Å. This is in good agreement with previous reports [10] and the pattern in figure 2(a) closely matches that of phase-pure samples of references [5] and [9]. The MP sample has already been well characterized in previous reports [5].

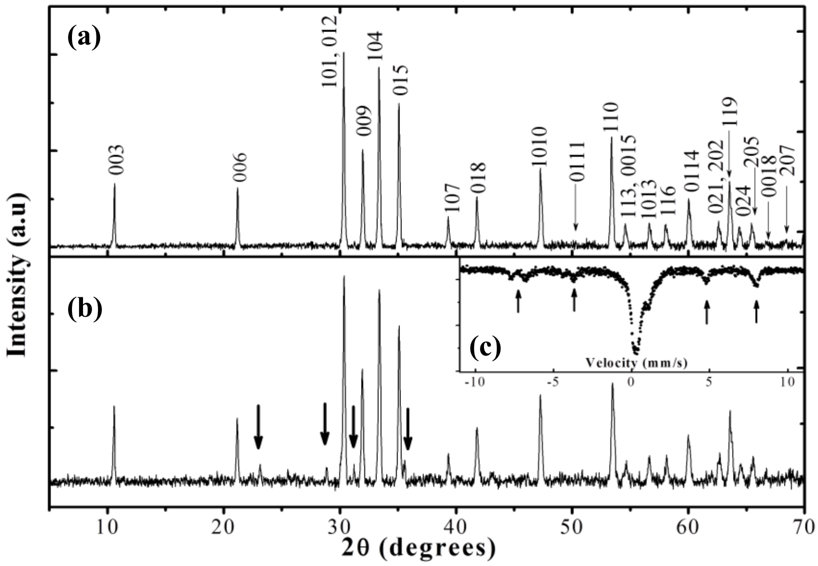

Figure 2 (colour online): XRPD data for (a) 100 mg and (b) 20 mg enriched $LuFe_2O_4$ pellets. Inset (c) shows the MES spectrum of the 20 mg sample. Arrows indicate impurity phases.

3.2. MES

Mössbauer spectra are shown for the MP and ^{57}Fe-enriched 100 mg samples at room temperature in figure 3 and at 15 K in figure 4. At room temperature the spectra are commonly fitted as a combination of two doublets, corresponding to Fe^{2+} and Fe^{3+}, typical of the mixed-valence state [9]. However, for a best fit it was necessary to include a Fe^{3+}/Fe^{2+} electron-hopping (EH) component whilst allowing the isomer shifts and quadrupole splitting to correlate to those of the individual mixed-valence components. The fitting yields an electron exchange rate of ~2 MHz. This likely occurs at CO domain boundaries or may be a result of CO frustration in the triangular network of figure 1(b). The abundance of the EH component in both samples is appreciable (~20%) with the 100 mg sample (figure 3(b)) having a slightly smaller EH frequency in comparison with the MP sample. This is possibly due to the different oxygen stoichiometries in the two samples.

At 15 K (figure 4), where $T << T_N$, complex magnetic hyperfine structure is observed. The spectra were both fitted using six sextets allocating three potential sites for Fe^{3+} and two for Fe^{2+} [9], as well as a smeared Fe^{2+} component. This multiplicity of Fe sites is compatible with the known ferrimagnetic structure of the compound and the Fe^{2+} and Fe^{3+} superstructure (CO) that occurs in each sheet of a bi-layer depicted in figure 1(a), as delineated in reference [4]. The model for each spectral component is calculated by solving the static Hamiltonian for mixed magnetic and quadrupole interactions using MOSSWINN [11]. The smeared component (broad linewidth, see last line of table 1) is supposed to originate from disordered spins (fluctuating or a distribution of B_{hf} values), anticipated to occur in such a frustrated network, see figure 1(b). Longer-range magnetic exchange interactions within the bilayers give rise to the spin aligned (ordered) components. The parameters derived from the fitting of the MES spectra at 15 K are shown in table 1 and confirm that distinct charge states, mixed-valence Fe^{3+} and Fe^{2+}, occur; as compared to parameter values typical of ferrous and ferric iron [12]. It is interesting to note that the disordered spins comprise mainly Fe^{2+} moments.

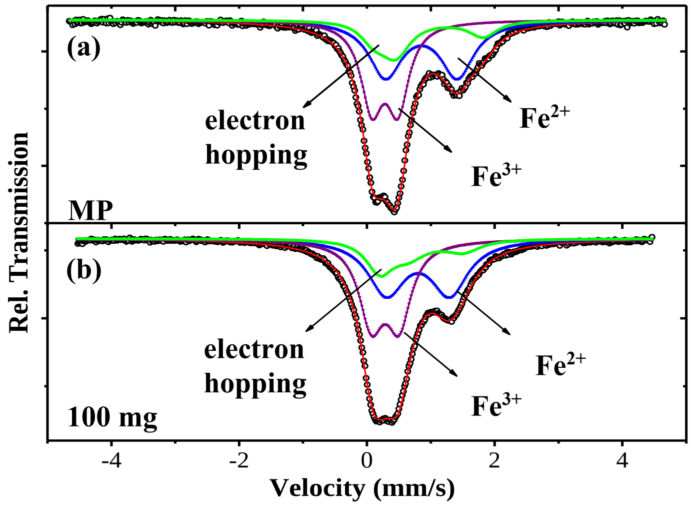

Figure 3 (colour online): Mössbauer spectra at RT for: (a) MP sample and (b) enriched 100 mg pellet.

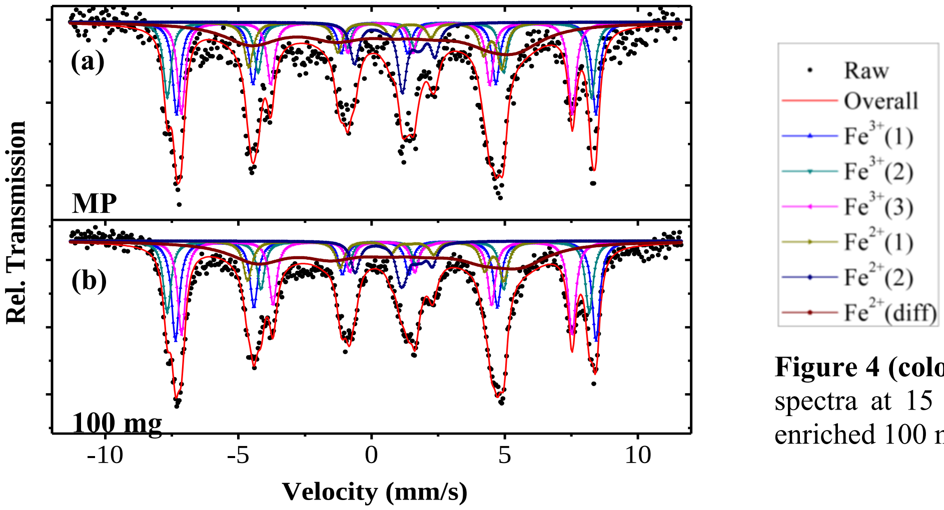

Figure 4 (colour online): Mössbauer spectra at 15 K for (a) MP and (b) enriched 100 mg pellet.

Table 1: MES parameters for the spectrum of the MP sample at 15 K. The isomer shift is δ and Beta is the angle between the electric field gradient V_{zz} and the internal magnetic field at the Fe site, B_{hf}. A very similar tabulation has been obtained for the enriched 100 mg sample.

Site	Γ line width[a] (mm/s)	δ / Fe (mm/s)	B_{hf} (T)	$V_{zz} \times 10^{21}$ (V/m^2)	$\lvert 1/2 \cdot eQV_{zz} \rvert$ (mm/s)	Beta (deg)	Abundance (%)
Fe^{3+} (1)	0.35	0.46	49	2.65	0.44	0	18
Fe^{3+} (2)	0.35	0.45	50	-0.33	0.05	0	14
Fe^{3+} (3)	0.35	0.39	45	-7.70	1.28	51	18
Fe^{2+} (1)	0.41	0.93	29	-8.20	1.37	5	10
Fe^{2+} (2)	0.41	1.13	6	-8.90	1.48	26	10
Fe^{2+} (diff)	2.5	1.13	31	-6.50	1.08	0	30

[a] Fixed parameters

3.3. *Magnetic susceptibility*

Zero-field cooled magnetic susceptibility measurements on warming are given in figure 5 for the three samples. T_N has been determined from the point of inflection on the high temperature side of the peak. The 20 mg pellet shows a T_N of 247 K as well as a higher magnetic ordering volume, indicative of the impurity phases present. The 100 mg and MP sample show curves with a T_N of 249 and 255 K, respectively. The differences in T_N are due to differences in oxygen stoichiometry δ of the two samples [5-7]. The MP sample has $\delta \sim 0$ and the decrease in T_N in the enriched sample is attributed to a slight oxygen deficiency [7], which is in the process of being quantified by means of TGA measurements. The as received MP sample shows an additional transition at ~210 K believed to be a stabilization of one of the degenerate magnetic configurations [13]. This evidently does not occur in the off-stoichiometric sample.

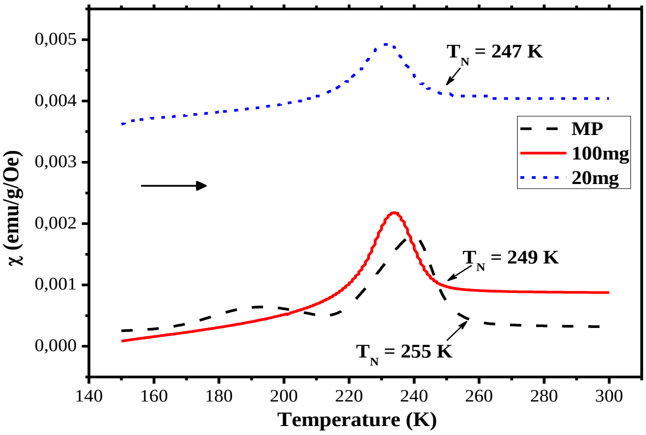

Figure 5 (colour online): Magnetic susceptibility for the ^{57}Fe-enriched 20 and 100 mg samples, as well as for the MP sample.

3.4. *TEM and ED*

In the numerous papers devoted to this ferrite, ED patterns along the [100] axis are characterized by additional reflections leading to commensurate or incommensurate modulation vectors; all the authors agree that they are the signatures of CO [5, 10]. ED from high resolution TEM studies were taken for the 100 mg ^{57}Fe enriched sample and compared to the as received MP sample.

Along the [100] axis in the MP sample (figure 6(a)), three modulation vectors are observed: $\mathbf{q}_2$ $(1/3\text{-}\varepsilon\ \ 1/3\text{-}\varepsilon\ \ 1/3)$, $\mathbf{q}_2$**’** by twinning and $\mathbf{q}_3$ (1/3 1/3 ½). The point-like satellites are rather intense, however weaker or rather diffuse satellites are also observed due to the *C2/m* sub-cell of *R3-m* [5]. Similarly, in the 100 mg enriched sample (figure 6(b)) weak zigzagging diffuse lines are observed (highlighted by the red arrows), which are associated with the $\mathbf{q}_2$, $\mathbf{q}_2$**’** and $\mathbf{q}_3$ vectors previously reported. This is similar to the MP samples (likely with short range charge ordered domains); except more intense satellites are present in the MP sample.

Along [010], the ED patterns of the 100 mg (figure 6(c)) and MP samples exhibit either no extra reflections, consistent with the *C2/m* structure, or there are satellites associated with an incommensurate modulated structure. The latter ones have been shown to be correlated with the formation of “oxidized” domains present in the matrix [5]; thus considered to be a true signature of a local excess of oxygen. The 100 mg sample thus shows an inhomogeneous distribution of oxygen throughout the lattice, as is the case in the MP sample (not shown here).

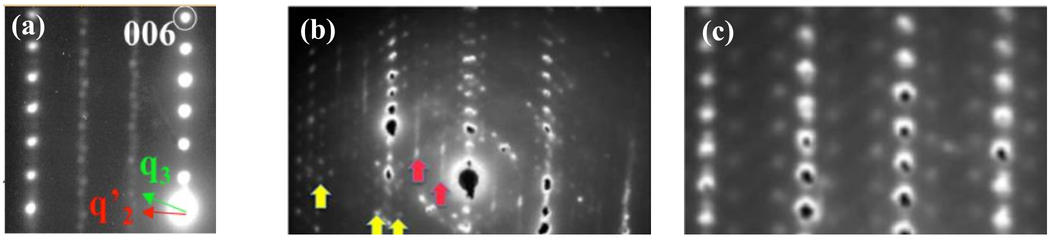

Figure 6 (colour online): ED patterns of (a) MP sample and (b) 100 mg enriched sample, along the [100] axis. Satellites from CO superstructure are emphasized by the red arrows; these are more intense in (a) and much weaker but nevertheless discerned in (b). Yellow arrows indicate unknown point-like satellites. (c) ED pattern for the 100 mg enriched sample along the [010] axis, showing satellites correlated to locally oxidized domains.

4. Conclusions

We are able to prepare small quantities of ^{57}Fe isotopically enriched mixed-valence $LuFe_2O_{4-\delta}$ samples in which CO prevails. Such isotopic enrichment is imperative for future envisaged MES studies under high pressure. These are phase pure materials when a minimal amount of ~100 mg is synthesized; there are slight deviations of oxygen stoichiometry from ideal δ~0 values. Oxygen stoichiometry may readily be altered by a mild heat treatment (150 - 200 °C) in air [5]. In both stoichiometric and off-stoichiometric samples oxygen is inhomogeneously distributed in the lattice; there being oxidized domains with a local excess of oxygen. The degree of off-stoichiometry does not drastically alter the magnetic-electronic properties as exemplified by the magnetization and Mössbauer characterizations. These results have been compared to those for a well-characterized reference sample (δ~0).

We have conducted a more comprehensive data analysis of the Mössbauer spectra than in the previous literature. The effects of geometrical charge and spin frustration, anticipated for such a triangular networked lattice structure, have been discerned in this detailed analysis by way of a residual electron-hopping component at $T < T_{CO}$ and disordered spins at $T << T_N$, respectively.

References

[1] Bibes M and Barthélémy A 2008 *Nat. Mater.* **7** 425-6
[2] Béa H, Gajek M, Bibes M and Barthélémy A 2008 *J. Phys.: Condens. Matter* **20** 434221 (1-11)
[3] Ikeda N, Ohsumi H, Ohwada K, Ishii K, Inami T, Kakurai K, Murakami Y, Yoshii K, Mori S and Horibe Y 2005 *Nature* **436** 1136 (1 - 3)
[4] Angst M 2013 *Phys. Status Solidi RRL* **7** 383-400
[5] Hervieu M, Guesdon A, Bourgeois J, Elkaïm E, Poienar M, Damay F, Rouquette J, Maignan A and Martin C 2014 *Nat. Mater.* **13** 74-80
[6] Wang F, Kim J, Gu G D, Lee Y, Bae S and Kim Y-J 2013 *J. Appl. Phys.* **113** 063909 (1 - 7)
[7] Yang H X, Tian H F, Wang Z, Qin Y B, Ma C, Li J Q, Cheng Z Y, Yu R and Zhu J 2012 *J. Phys.: Condens. Matter* **24** 435901 (1 - 7)
[8] Xu X, Angst M, Brinzari T, Hermann R P, Musfeldt J, Christianson A D, Mandrus D, Sales B, McGill S and Kim J-W 2008 *Phys. Rev. Lett.* **101** 227602 (1 - 4)
[9] Bang B K, Kouh T and Kim C S 2008 *J. Appl. Phys.* **103** 07E307 (1 - 3)
[10] Rouquette J, Haines J, Al-Zein A, Papet P, Damay F, Bourgeois J, Hammouda T, Doré F, Maignan A and Hervieu M 2010 *Phys. Rev. Lett.* **105** 237203 (1 - 4)
[11] Klencsár Z 2013 Mössbauer fitting program: *MOSSWINN* 4.0 http://www.mosswinn.com/
[12] Gütlich P, Bill E and Trautwein A X 2011 *Mössbauer Spectroscopy and Transition Metal Chemistry: Fundamentals and Applications* (Berlin: Springer)
[13] Christianson A D, Lumsden M D, Angst M, Yamani Z, Tian W, Jin R, Payzant E A, Nagler S E, Sales B C and Mandrus D 2008 *Phys. Rev. Lett.* **100** 107601 (1 - 4)

Reply to referees' comments – SAIP 2014 Conference proceedings

Article ID 82, MA Peck et al.

Dear Editor

On behalf of all the co-authors, I would like to thank the referees for their comments and suggestions on our manuscript; these have helped to improve the presentation of our results. I would also like to thank the SAIP2014 Editorial Board for processing the reviewing of our manuscript.

We have revised the manuscript according to the suggestions. Please find below the detailed answers to the referees' questions and concerns. (Referees' questions are shown in red, while our reply is in black.)

Kind Regards,
M Adli Peck
(On behalf of all co-authors)

===

REFEREE 1:

1. Please move some text around so that table 1 does not span across two pages. This has been implemented.

2. Please bring the 'References' heading in line with the other headings. This has been implemented.

===

REFEREE 2:

1. Define TN –whenever using a symbol for the first time, it must be described fully. This has been changed in the abstract to "onset of ferrimagnetic ordering is ...." It is already defined in Section-1 (Introduction) second paragraph line-6 and third paragraph line-13.

2. Plenitude or plentitude – I am not sure of the meaning of the word –please check, possibly just my ignorance. Section-1 (Introduction) second paragraph line-2: "a plenitude of degenerate charge and ..." has been changed to "a number of degenerate charge and ..."

3. TEM- explain. Abstract, line-3: "… TEM/electron-diffraction …" has been changed to "…. transmission electron microscopy as well as electron-diffraction …"
Introduction, 3rd paragraph, line-3: "… TEM and electron diffraction (ED) …" has been changed "… transmission electron microscopy (TEM) and electron diffraction (ED)…" Furthermore, sub-section 3.4, line-1 of the first paragraph has been modified to "ED".

4. TCO – explain. Section-1 (Introduction), third paragraph line-11: "… occurs below Tco = 320 K ..." has been amended to "… occurs below an onset temperature of Tco = 320 K ..."

5. Figure 2: Please index all peaks. These have been implemented in figure 2 (a), see also reference [5].

===

REFEREE 3:

1. Sample quality: The detrimental influence of impurity phases and deviation from stoichiometry in the subject materials makes it compelling that the authors should also illustrate: (i) the results of Rietveld profile refinement (ii) the diffraction spectrum of sample MP which is claimed to be of good quality. In case of (i): the full Rietveld profile and its comparison with the experimental pattern (difference plot) has been omitted for the sake of brevity. The indexing of the peaks has been included in figure 2 (a) and the pattern shows an identical match to those of phase-pure compounds in references [5] and [9]. Also see sub-section 3.1, second paragraph lines 2 and 3, which we have modified to read as: "This is in good agreement with previous reports [10] and the pattern in figure 2 (a) closely matches that of phase-pure samples of references [5] and [9]." In case of (ii): Sample MP has been obtained via one of the co-authors Dr C. Martin (Caen-France). This sample has been extensively characterised in previous studies, see references [5] and [10]. This is also mentioned in Section-2 (Experimental), paragraph one, lines 6 – 8. Again, for the sake of brevity, we do not reproduce that previous characterisation here.

2. Fig 2(b) and (c): Unless the authors can clarify the nature or composition of the impurity phases marked with arrows, the reviewer's judgement is that any conclusions drawn from this 20 mg sample are flawed and detract from the scientific value of the study. See explanation in sub-section 3.1, first paragraph. Impurity phases of figure 2(b) and 2(c) only

occur when samples are made in very small quantities. This is one of our important findings, namely that to ensure impurity phases are below (XRD and Mossbauer) detection levels (of typical ~5% abundance), minimum quantities of ~100 mg of sample need to be synthesized for this compound, as depicted in figure 2(a) and figure 3(b). From the Mossbauer spectrum of figure 2(c) remnant magnetite (Fe_3O_4) has been identified as an impurity phase.

We have made the following amendments (additions):

Sub-section 3.1 first paragraph, lines 2-3: "Sample MP's diffraction pattern (not shown here) …" now reads: "Sample MP's diffraction pattern (not shown here, see reference [5]) …"

First paragraph line-6 : " … which shows remnant evidence of Fe_3O_4 and Fe impurity phases (as indicated by arrows), not …" now reads "… which shows evidence of remnant Fe_3O_4 and Fe impurity phases (as indicated by arrows) from the reaction sequence, not …"

3. A major claim of the work is the finding of a mixed-valence state and charge and spin frustration in the title compound.

(i) The authors should clarify the [crystal structure] site multiplicity of Fe, and whether this multiplicity is affected by purposeful changes in the oxygen stoichiometry.

Similarity of spectra in figure 4(a) and (b) for stoichiometric and slightly off-stoichiometric (enriched) samples, respectively, indicates that site multiplicity is evidently not affected drastically by changes in stoichiometry. This is already alluded to in the Conclusions (line 7). All Fe^{2+} sites and all Fe^{3+} sites are crystallographically similar to each other as reflected in the non-magnetic spectra of figure 3(a) or (b), where, for example, a single sub-spectrum may be used to represent all Fe^{2+} sites and similarly for Fe^{3+}. These sub-components are more readily distinguishable from each other in the magnetic spectra of figures 4(a) or (b), due to the superior spectral resolution offered by the magnetic hyperfine splitting.

We have added a sentence to clarify this, see sub-section 3.2, second paragraph, line-3. The sentence added reads: "This multiplicity of Fe sites is compatible with the known ferrimagnetic structure of the compound and the Fe^{2+} and Fe^{3+} superstructure (CO) that occurs in each sheet of a bi-layer depicted in figure 1(a), as delineated in reference [4]."

(ii) bottom of page 3, last paragraph: the authors state to have used three potential sites for Fe^{3+} and two sites for Fe^{2+}, plus an additional 'smeared' Fe^{2+} component; can the authors clarify whether the mixed-valence claim of this paper refers to an attribute of heterogeneous distribution of the two iron species or an attribute of chemical site multiplicity;

See previous response above and our addition to sub-section 3.2, second paragraph, and line-3. This is a chemical site multiplicity in the form of a superstructure (for example, Fe^{2+}-Fe^{3+}-Fe^{2+}-…), so as to minimize the Coulomb repulsion. Hence, the Bragg satellites depicted in Figure 6, as a result of this charge density wave.

(iii) Page 4, paragraph 1: the authors conclude that "... it is interesting to note that the disordered spins comprise mainly Fe2+ moments". Qualify "disordered" in this sentence; e.g. are these paramagnetic spins, frustrated spins or crystallographic site disordered spins in this sentence. Unless the latter is the case, what evidence do the authors have for the disordered nature of the spins?

We are referring to frustrated spins, as this would be anticipated in the triangular network of the crystal structure, see figure 1(b). This has already been alluded to in sub-section 3.2, second paragraph, line-5 onwards. The disordered nature of the spins is deduced from the broad linewidth (last line of table-1) associated with this component, indicative of a fluctuating magnetic hyperfine field or distribution of B_{hf} values.

Sub-section 3.2, second paragraph, line-7 onwards. We have modified the sentence: "The smeared component is …" to read: "The smeared component (broad linewidth, see last line of table 1) is supposed to originate from disordered spins (fluctuating or a distribution of Bhf values), anticipated to occur in such a frustrated network, see figure 1(b)."